J. Plasma Physics (2011), *vol.* 77, *part* 5, *pp.* 639–651.
doi:10.1017/S0022377811000018

Microwave shielding of HiPco carbon nanotube films

AFSHIN MORADI[1,2] and
MOHAMMAD HOSAIN TEIMOURPOUR[1]

[1]Department of Nano Science, Kermanshah University of Technology, Kermanshah, Iran
[2]Department of Nano Science, Institute for Studies in Theoretical Physics and Mathematics (IPM), Tehran, Iran
(a.moradi@nano.ipm.ac.ir)

(Received 20 October 2010, revised 3 December 2010 and accepted 4 January 2011; first published online 3 February 2011)

Abstract. The theoretical study of microwave characteristics of a thin film of hydrogen plasma in carbon nanotubes, which were grown by iron-catalyzed high-pressure carbon monoxide disproportionation, is presented. The system is assumed to be illuminated by either a transverse magnetic (TM) or a transverse electric (TE) waves at an arbitrary angle of incidence to the film. By considering the interference effects because of multiple reflections between thin plasma layer interfaces, the reflectance, transmittance, and absorptance of microwave radiation at the plasma film are deduced and their functional dependence on the continuous changing of the angle of propagation and plasma thickness with fixed parameters of the system are studied. The simulation results show that for the present system, the interference effects lead to a sinusoidal variation of the reflected intensity and can greatly reduce the amount of reflection power, but the absorption power increases. In addition, it is found that the TE and TM waves have largely indistinguishable microwave absorption and transmission spectrums.

1. Introduction

The interaction of microwaves with carbon nanotubes (CNTs) is an interesting topic for a variety of potential applications. Some basic studies have focused on understanding the nature of the interactions between radiation and CNTs, while the observed behavior has been used for many exciting purposes. For instance, Li and Lue [1] proposed a novel method of measuring the dielectric constants of single-wall CNTs by using a microwave dielectric resonator. Also, CNTs have been confirmed as good candidates for ultrasensitive gas sensors because of the high surface to volume ratio of nanostructures and their distinctive electrical properties [2].

While there is still a need to investigate the mechanism of CNT–microwave interactions [3], when CNTs are exposed to microwaves, strong absorptions are observed [4], producing intense heating, outgassing, and light emission. However, another potential source of localized superheating should be considered, namely, the generation of gas plasma from absorbed gases (particularly H_2) in CNTs under microwave radiation [4]. Hydrogen is adsorbed inside the nanotubes or between the bundles of nanotubes, or on the surfaces of nanotube bundles [5]. The

experiments show that condensing capacity of hydrogen on CNTs increases with pressure increasing or temperature dropping down. Moreover, metallic nanoparticles are favorable for hydrogen adsorption of CNTs[6].

Carbon nanotubes produced via high-pressure carbon monoxide disproportionation (HiPco) process have been extensively explored for potential applications in electromagnetic shielding or absorbing materials [7–13]. The production of iron-catalyzed HiPco-grown single-walled carbon nanotubes (SWCNTs) [14, 15] studied and optimized with respect to a number of process parameters, including temperature, carbon monoxide pressure, and $Fe(CO)_5$ catalyst concentration. The adsorbed hydrogen on HiPco CNTs may have come from the laboratory environment or being produced via iron-catalyzed decomposition of water and organic pyrolysate materials (such as solvent or pump oil) [4]. Wadhavan and co-workers [7] compared the behavior of raw and purified HiPco CNTs and concluded that microwave energy is predominantly absorbed by the magnetic resonance among iron catalyst particles. Naab and co-workers [8] repeated the experiments of Refs. [4] and [7] under the same microwave field conditions, using a particle-induced X-ray emission (PIXE) experiment, and showed that metallic impurities do not play a predominant role for the absorption of microwave energy in CNTs.

Microwave interaction with HiPco SWNTs under high vacuum ($\sim 10^{-6}$ torr) generates highly ionized hydrogen plasma. With plasma emergence the effects of microwave nanotubes interaction appear as a result of the interaction between highly ionized hydrogen plasma. Consequently, it provides an independent mechanism for absorbing microwave energy, and it can be possible to model this subject from the perspective of plasma physics. In this way, Peng et al. [9, 10], by using the fluid theory, the Lambert-Beer law, and the WKB approximation, investigated the microwave loss mechanisms of hydrogen plasma in HiPco CNTs, theoretically. The experimental phenomenon of strong microwave absorption (around 2.45 GHz) by HiPco CNTs was well explained by Peng's model. Also, we derived simple sets of equations to describe the microwave response of the magnetized uniform hydrogen plasma slab in HiPco CNTs [11–13].

However, in previous works [9–13], there is a fundamental assumption, where it is assumed that the thickness of plasma d is larger than the wavelength of incident wave λ (*i.e.* d is thicker than the coherence length of the light). When the plasma thickness is very thin (for example, the thickness of plasma slab is near or much less than the order of the wavelength of incident wave), the interference effects [16–19] in the response to the optical spectrums of the system have to be considered.

In this paper, we investigate the propagation property of the electromagnetic wave in a thin hydrogen plasma layer in the presence of CNTs, where the value of d/λ is less than 2 and focus on the effects of interference on microwave response of the system. For the first time, both polarizations of the incident transverse magnetic (TM) and transverse electric (TE) waves will be treated. We will further call this treatment the coherent description of the multiple reflections as opposed to the incoherent description in (3) to (11) in our previous work [12]. In particular, we study functional dependence of the reflectance, transmittance, and absorptance on the continuous changing of the angle of propagation and plasma thickness with fixed parameters of the system.

https://doi.org/10.1017/S0022377811000018 Published online by Cambridge University Press

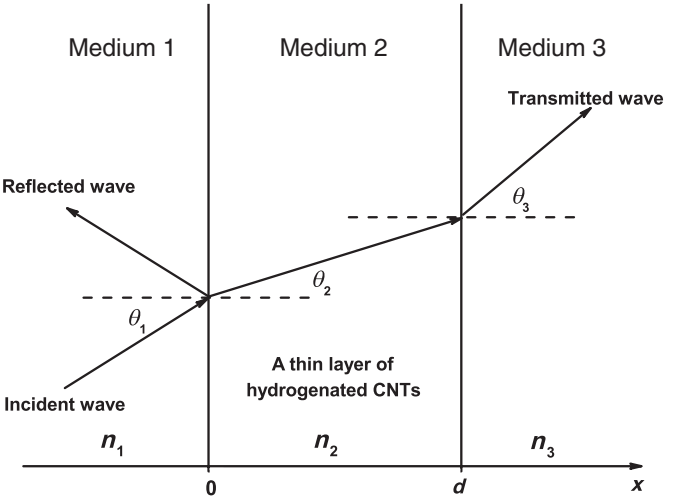

Figure 1. Schematic representation of the hydrogen plasma slab characterized by its thickness d.

2. Theoretical model

As has been mentioned above that the previous investigation [12] based on the involved light intensities is correct only if the plasma slab is thicker than the coherence length of the light. In this work, by considering the interference effects, we shall treat the microwave response of the isotropic and homogeneous hydrogen plasma slab in the presence of CNTs.

The dielectric structure is described by Gradov and Stenflo [20]

$$n(x) = \begin{cases} n_1, & x < 0, \\ n_2, & 0 < x < d, \\ n_3, & \mathrm{d} < x, \end{cases} \tag{2.1}$$

where n_1, n_2, and n_3 are the refractive indices and the plasma slab is further characterized by its thickness d (see Fig. 1). Optical and dielectric properties of the hydrogen plasma slab in the presence of CNTs can be characterized by a complex refractive index

$$n_2 = n - i\kappa, \tag{2.2}$$

where n is the real and κ is the imaginary part of the refractive index. κ is also often denoted as extinction coefficient.

The hydrogen plasma in the presence of CNTs can be characterized by the effective complex permittivity $\varepsilon_r = n_2^2 = \varepsilon_r' - i\varepsilon_r''$ [11–13], as

$$\varepsilon_r = 1 - \frac{\upsilon_p^2}{\upsilon^2 + \upsilon_e^2} - i\frac{\upsilon_p^2 \upsilon_e}{\upsilon\left(\upsilon^2 + \upsilon_e^2\right)}, \tag{2.3}$$

where

$$\upsilon_p = \sqrt{\frac{(n_{e,\mathrm{plasma}} + n_{e,\mathrm{CNTs}})e^2}{\varepsilon_0 m_e}}$$

https://doi.org/10.1017/S0022377811000018 Published online by Cambridge University Press

is the plasma frequency and $\upsilon_e = \upsilon_{e,\text{plasma}} + \upsilon_{e,\text{CNTs}}$ is the effective collision frequency between electrons and neutral plasma particles, and between electrons and CNTs. $n_{e,\text{plasma}}$ and $n_{e,\text{CNTs}}$ are the electron density of hydrogen plasma and electron density of CNTs, respectively.

Since the whole medium is homogeneous in the z direction (*i.e.* $\partial n/\partial z = 0$), the electric field vector of a general plane-wave solution of the wave equation can be of the form

$$\mathbf{E} = \mathbf{E}(x)\exp[i(\omega t - \beta z)], \tag{2.4}$$

where the parameter β is the z component of the propagation wave vector and ω is the angular frequency. In (4), we assume that the microwave is propagating in the $x-z$ plane and the electric field is either an s wave (with $\mathbf{E}\|\mathbf{y}$) or a p wave (with $\mathbf{H}\|\mathbf{y}$). Using the Maxwell's curl equation, $\mathbf{H} = -(i\omega\mu)^{-1}\nabla\times\mathbf{E}$, the corresponding tangential magnetic field components of (4) can be obtained. The boundary conditions on the tangential components of the electric and magnetic field vectors require that E_y, E_z, H_y, and H_z must be continuous at the interfaces $x = 0$ and $x = d$ [16–18]. Since the field vectors must satisfy the boundary conditions at the interfaces, β must have the same value in all the layers, so that the relation between θ_1, θ_2, and θ_3 is given by Snell's law:

$$n_1 \sin\theta_1 = n_2 \sin\theta_2 = n_3 \sin\theta_3, \tag{2.5}$$

where θ_i, with $i = 1, 2, 3$, is the ray angle measured from the x-axis, as indicated in Fig. 1.

For the case of incidence from the left, the electric field vector $\mathbf{E}(x) = E_y(x)\hat{j}$ can be written as

$$E_y(x) = \begin{cases} Ae^{-ik_{1x}x} + Be^{ik_{1x}x}, & x < 0, \\ Ce^{-ik_{2x}x} + De^{ik_{2x}x}, & 0 < x < d, \\ Fe^{-ik_{3x}(x-d)}, & d < x, \end{cases} \tag{2.6}$$

where we assume that the electric field vector is s-polarized (TE wave) and

$$k_{ix} = \left[\left(\frac{n_i\omega}{c}\right)^2 - \beta^2\right]^{1/2} = \frac{\omega}{c}n_i\cos\theta_i, \qquad i = 1, 2, 3, \tag{2.7}$$

is the x component of the wave vectors. The unknown complex amplitudes A, B, C, D, and F can be found by applying the appropriate boundary conditions. For the case of s wave, the boundary conditions require that E_y and H_z be continuous at the interfaces. The z component of the magnetic field is obtained by using $H_z = (i/\omega\mu)(\partial E_y/\partial x)$ and is given by

$$H_z(x) = \begin{cases} \dfrac{k_{1x}}{\omega\mu}(Ae^{-ik_{1x}x} - Be^{ik_{1x}x}), & x < 0, \\ \dfrac{k_{2x}}{\omega\mu}(Ce^{-ik_{2x}x} - De^{ik_{2x}x}), & 0 < x < d, \\ \dfrac{k_{3x}}{\omega\mu}Fe^{-ik_{3x}(x-d)}, & d < x. \end{cases} \tag{2.8}$$

Imposing the continuity of E_y and H_z at the interfaces $x = 0$ and $x = d$, and doing some algebra, the reflection and transmission coefficients can be written as

$$r = \frac{r_{12} + r_{23}e^{-2i\phi}}{1 + r_{12}r_{23}e^{-2i\phi}}, \tag{2.9}$$

https://doi.org/10.1017/S0022377811000018 Published online by Cambridge University Press

and

$$t = \frac{t_{12}t_{23}e^{-i\phi}}{1 + r_{12}r_{23}e^{-2i\phi}}, \tag{2.10}$$

where the Fresnel reflection and transmission coefficients of the dielectric interfaces are given by

$$r_{\ell m} = \frac{k_{\ell x} - k_{mx}}{k_{\ell x} + k_{mx}}, \tag{2.11}$$

$$t_{\ell m} = \frac{2k_{\ell x}}{k_{\ell x} + k_{mx}}, \tag{2.12}$$

with $\ell = 1, 2$ and $m = \ell + 1$. The parameter ϕ in (9) and (10) is given by

$$\phi = k_{2x}d = \frac{2\pi d}{\lambda} n_2 \cos\theta_2, \tag{2.13}$$

and is proportional to the thickness d and the index n_2 of the layer. A similar electromagnetic analysis for p-polarized (TM wave) leads to exactly the same (9) and (10) for the transmission and reflection coefficients, respectively, except that the coefficients t_{12}, t_{23}, and r_{12} and r_{23} are given by

$$r_{\ell m} = \frac{n_\ell^2 k_{mx} - n_m^2 k_{\ell x}}{n_\ell^2 k_{mx} + n_m^2 k_{\ell x}}, \tag{2.14}$$

$$t_{\ell m} = \frac{2n_\ell^2 k_{mx}}{n_\ell^2 k_{mx} + n_m^2 k_{\ell x}}. \tag{2.15}$$

With the above equation, we will present the simulation results of the reflectance, transmittance and absorptance of microwave radiation by thin hydrogen plasma slab in the presence of CNTs.

3. Numerical result and discussion

In this section, with the above equation, we present the simulation results of the reflectance, transmittance, and absorptance of microwave radiation by system and investigate their dependence on the continuous changing of the angle of propagation and plasma thickness with fixed parameters of the system. Before the calculation, we need to determine the designed plasma parameters such as plasma density $n = n_{e,\text{plasma}} + n_{e,\text{CNTs}}$ and the effective collision frequency υ_e. Let us note that under normal conditions, the free electron density in plasma is generally 10^{17}–10^{19} m^{-3}, where we take n as the order of magnitudes of 10^{17} m^{-3}. The order of magnitudes of υ_e is usually 10^9–10^{10} Hz, and we take υ_e as the order of magnitudes of 10^9 Hz. Also, we assume that the thin slab is suspended in air so that we set $n_1 = n_3 = 1$. Let us note that reflectance is defined as the fraction of the energy reflected from the system and is given by

$$R = | r |^2, \tag{3.1}$$

and transmittance is given by

$$T = \frac{n_3 \cos\theta_3}{n_1 \cos\theta_1} | t |^2 . \tag{3.2}$$

https://doi.org/10.1017/S0022377811000018 Published online by Cambridge University Press

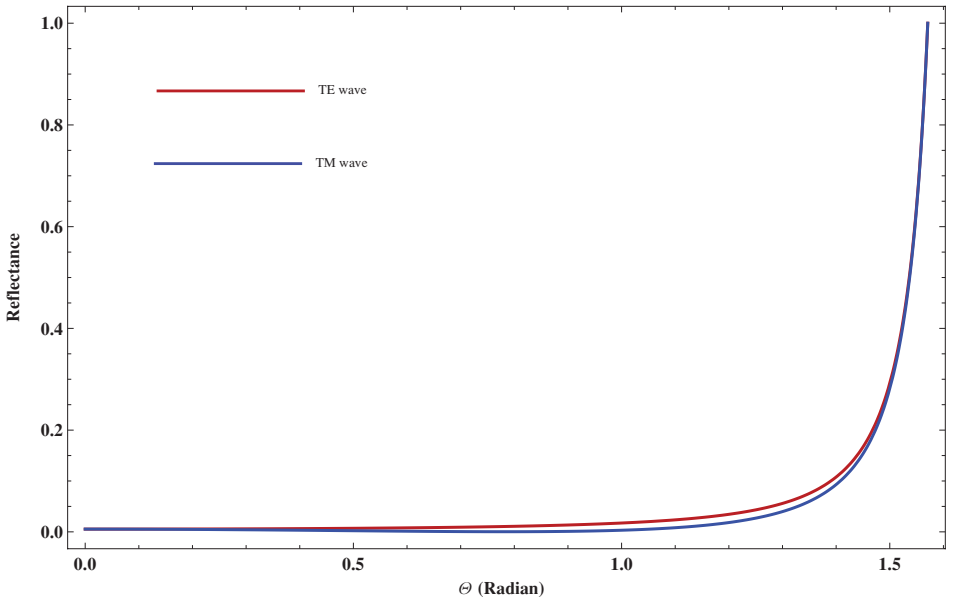

Figure 2. (Color online) Total reflected power versus incident angle of propagation for TM and TE waves, when $n = 2.181 \times 10^{17}$ m^{-3}, $\upsilon_e = 22$ GHz, $d = 1$ cm, and $\upsilon = 2.45$ GHz.

Likewise, absorptance, which is defined as the fraction of energy dissipated, is given by

$$A = 1 - R - T. \tag{3.3}$$

Figure 2, shows the total reflected power versus incident angle of propagation for TE and TM waves with the electron density $n = 2.181 \times 10^{17}$ m^{-3}, the collision frequency $\upsilon_e = 22$ GHz, the plasma slab width $d = 1$ cm, and the incident frequency $\upsilon = 2.45$ GHz. It can be seen that for both polarizations, the amount of reflection power is very low and the reflectance only increases with increasing the incident angle of propagation for $\theta > 70°$. The reflectance for both s and p waves as a function of d/λ, when $n = 2.181 \times 10^{17}$ m^{-3}, $\upsilon_e = 22$ GHz, and $\upsilon = 2.45$ GHz, is given in Fig. 3. The angle of propagation is arbitrarily chosen to be equal to 30°. It is clear that the interference effects lead to a sinusoidal variation of the reflected intensity for $d < 2\lambda$. Also, the reflectance of the s wave is greater than the reflectance of the p wave. By using the above plasma parameters, the dependence of the total transmitted power of plasma film versus incident angle and plasma slab width are exhibited in Figs. 4 and 5, respectively. As a consequence, the incident angle of propagation can greatly reduce the amount of transmittance of both polarizations for $d > 30°$. Note that the transmittance is insignificant for $d > 2\lambda$ and the TE and TM waves have quite the same transmission spectrums as for the present system. The dependence of the total absorbed power of hydrogen plasma slab versus incident angle of propagation for TE and TM waves with $n = 2.181 \times 10^{17}$ m^{-3}, $\upsilon_e = 22$ GHz, $d = 1$ cm, and $\upsilon = 2.45$ GHz is shown in Fig. 6. We see that for both polarizations, absorptance increases with increasing the incident angle of propagation and reaches a maximum at certain angles of incident. In order to see clearly the influence of the plasma slab width on the total absorbed power of hydrogen plasma slab, we plot the total absorbed

https://doi.org/10.1017/S0022377811000018 Published online by Cambridge University Press

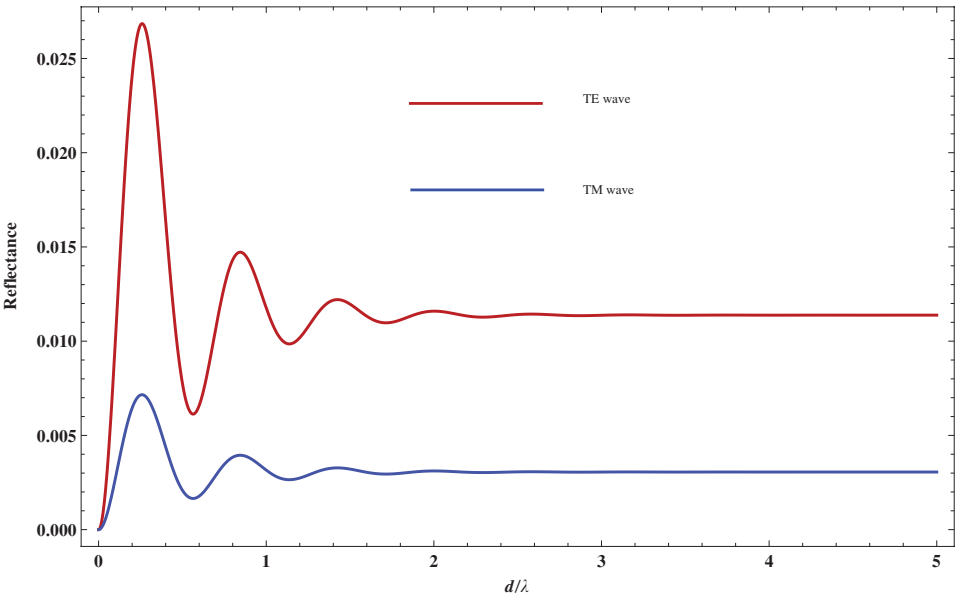

Figure 3. (Color online) Total reflected power versus plasma slab width for TM and TE waves, when $n = 2.181 \times 10^{17}$ m^{-3}, $\upsilon_e = 22$ GHz, $\theta = 30^{\circ}$, and $\upsilon = 2.45$ GHz.

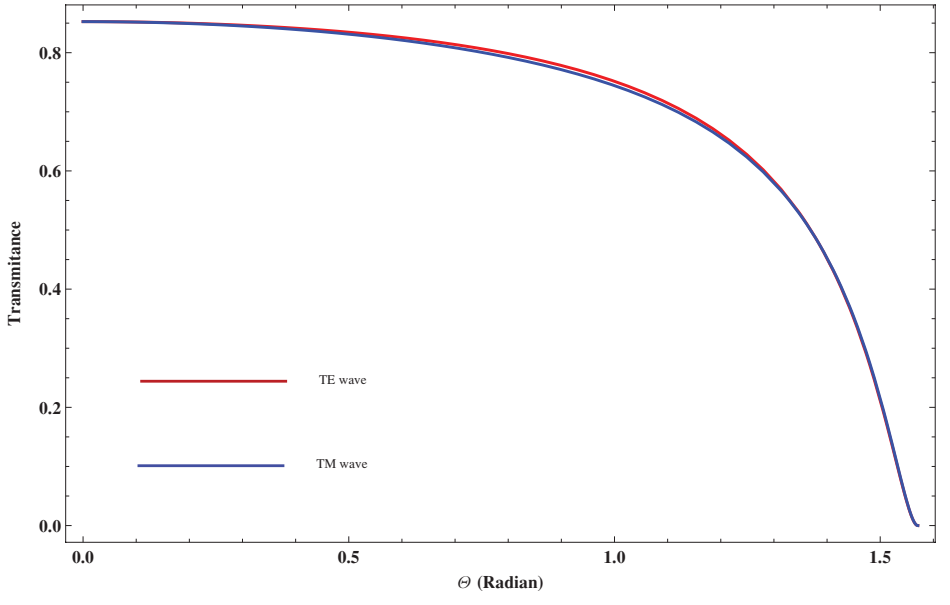

Figure 4. (Color online) Total transmitted power versus incident angle of propagation for TM and TE waves, when $n = 2.181 \times 10^{17}$m^{-3}, $\upsilon_e = 22$ GHz, $d = 1$ cm, and $\upsilon = 2.45$ GHz.

https://doi.org/10.1017/S0022377811000018 Published online by Cambridge University Press

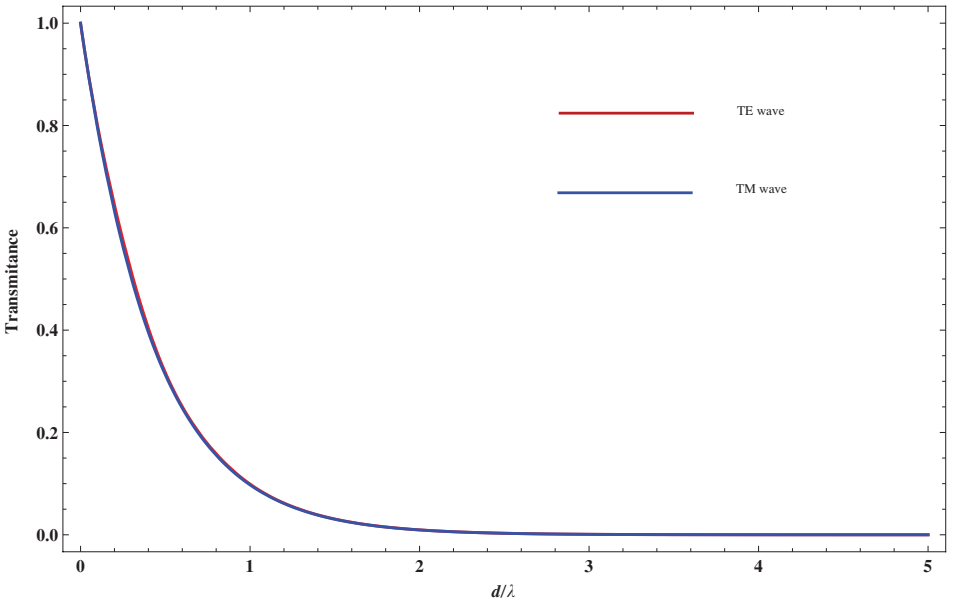

Figure 5. (Color online) Total transmitted power versus plasma slab width for TM and TE waves, when $n = 2.181 \times 10^{17}\mathrm{m}^{-3}$, $\upsilon_e = 22$ GHz, $\theta = 30^{\circ}$, and $\upsilon = 2.45$ GHz.

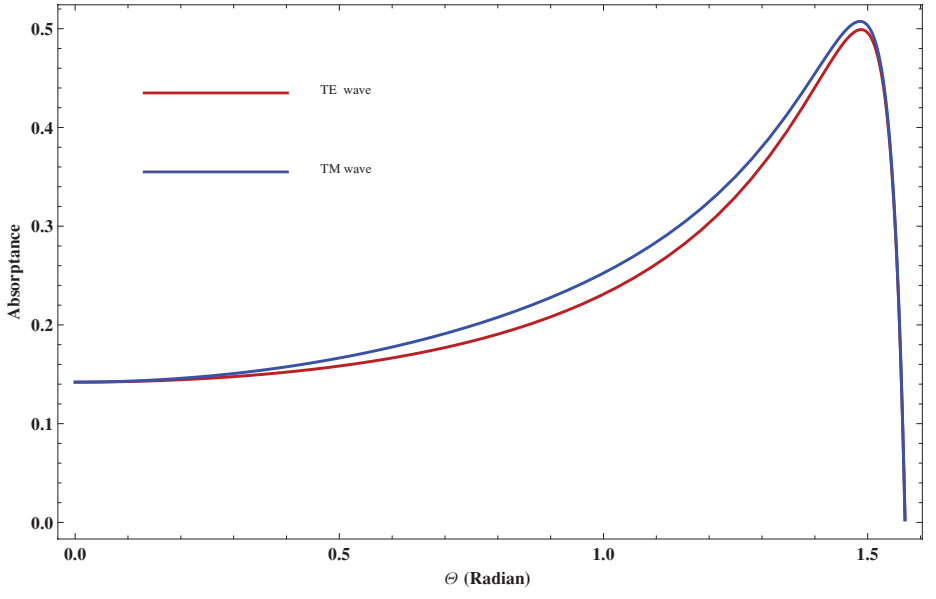

Figure 6. (Color online) Total absorbed power versus incident angle of propagation for TM and TE waves, when $n = 2.181 \times 10^{17}$ m^{-3}, $\upsilon_e = 22$ GHz, $d = 1$ cm, and $\upsilon = 2.45$ GHz.

https://doi.org/10.1017/S0022377811000018 Published online by Cambridge University Press

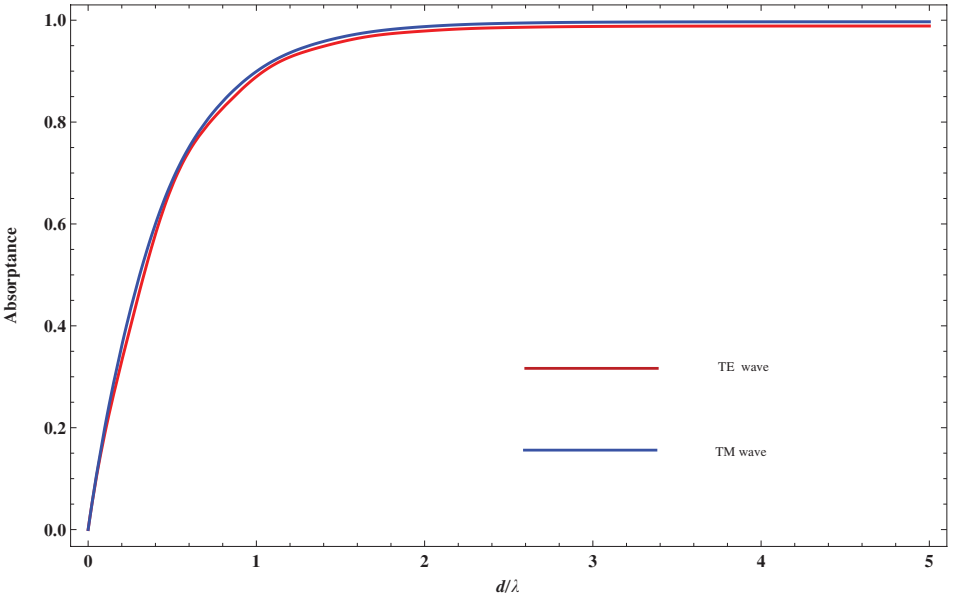

Figure 7. (Color online) Total absorbed power versus plasma slab width for TM and TE waves, when $n = 2.181 \times 10^{17}$ m^{-3}, $\upsilon_e = 22$ GHz, $\theta = 30°$, and $\upsilon = 2.45$ GHz.

power as a function of d/λ when $\theta = 30°$ as shown in Fig. 7. The absorptance is significant for $d > \lambda$ and the asymptotic behaviors of TE and TM waves are largely similar.

In order to investigate the interference effects because of multiple reflections between thin plasma layer interfaces, and compare the new results with the previous work [12], we now consider the common case of perpendicular incidence (θ_1 and $\theta_2 = 0$). In this case, there is no difference between s and p waves. In addition, let assume $n = 2.181 \times 10^{17}$ m^{-3}, $\upsilon_e = 22$ GHz, and $d = 1$ cm. Figures 8–10 show the dependence of reflection, transmission, and absorption of hydrogen plasma slab on microwave frequency by using (6)–(9) in Ref. [12], and considering the interference effects, respectively. One can see the fluctuations of reflected fields in Fig. 8(b); this sinusoidal variation of the reflected field reveals an interesting feature of the interference effect in microwave response of the system; in addition, it can be concluded that the interference effects can greatly reduce the amount of reflection power, where this result is quite different from the one given Ref. [21]. We note that for small periodic variations of the dielectric permittivity in metamaterials [21], however, the situation is radically different, and the coupling to leaking surface waves can then strongly influence the reflective properties, and in special conditions the incident wave energy is reflected in the backward direction.

Let note that if the slab thickness becomes longer than the coherence length, then we can simply add the intensities of the individual light beams to get the total intensity (as done in the derivation of (3) to (11) in Ref. 12), but here we have to add the amplitudes of the electric field strength observing the actual phase. However, it is easy to find that the reflectance curves of the hydrogen plasma slab (in the presence or absence of the interference effects) will approach each other for

https://doi.org/10.1017/S0022377811000018 Published online by Cambridge University Press

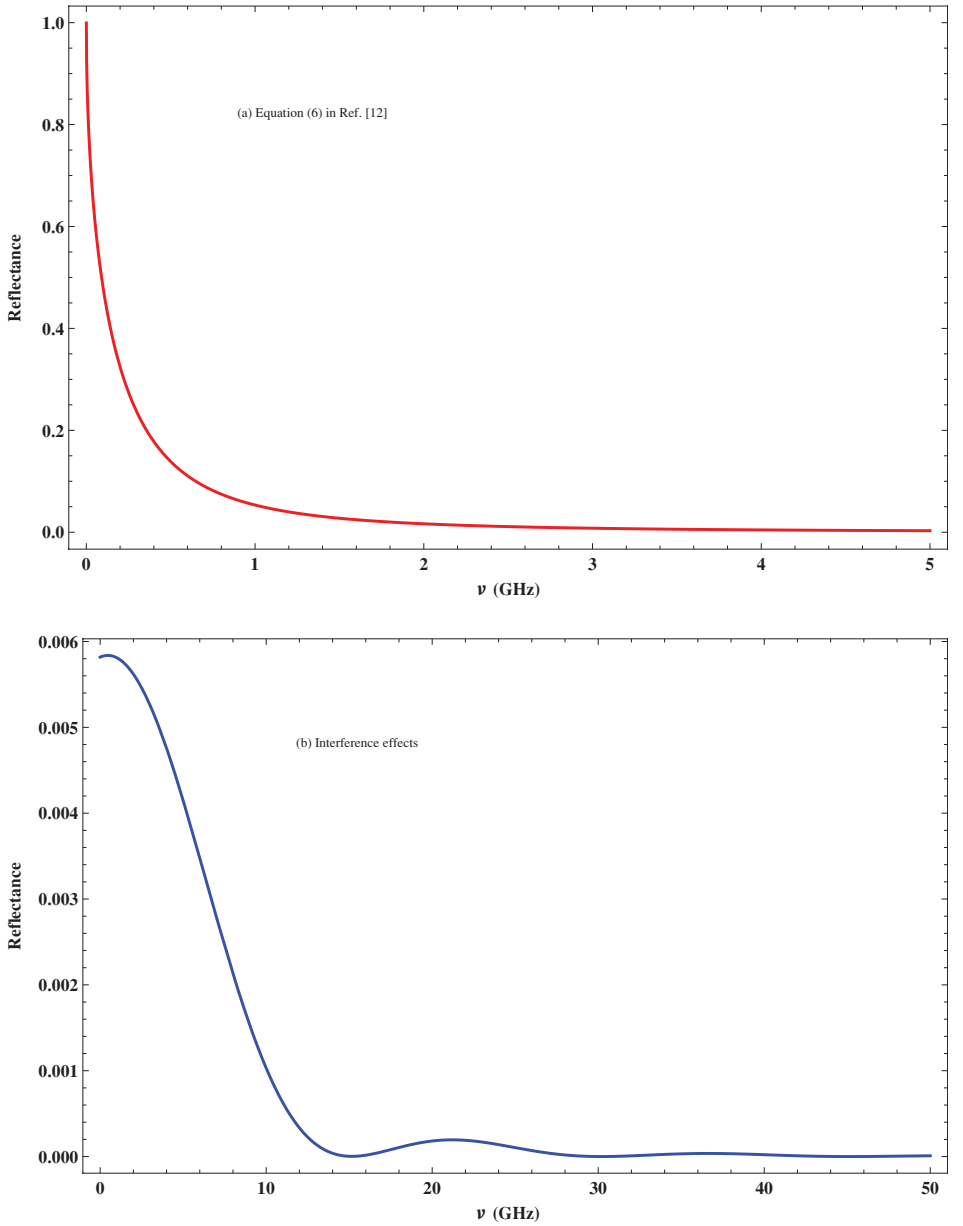

Figure 8. (Color online) Dependence of reflectance of hydrogen plasma slab on microwave frequency, when $n = 2.181 \times 10^{17}$ m^{-3}, $d = 1$ cm and $\upsilon_e = 22$ GHz. (a) from (6) in Ref. [12], (b) in the presence of interference effects.

$d > 3\lambda$. From Fig. 9, one can see that the interference effects can reduce the amount of transmission power. Finally, in Fig. 10 we see that the interference effects can greatly increase the amount of absorptance of the system. Thus, in practice, a very thin hydrogen plasma film in the presence of CNTs could be tailored to act as a absorber of microwave radiation.

https://doi.org/10.1017/S0022377811000018 Published online by Cambridge University Press

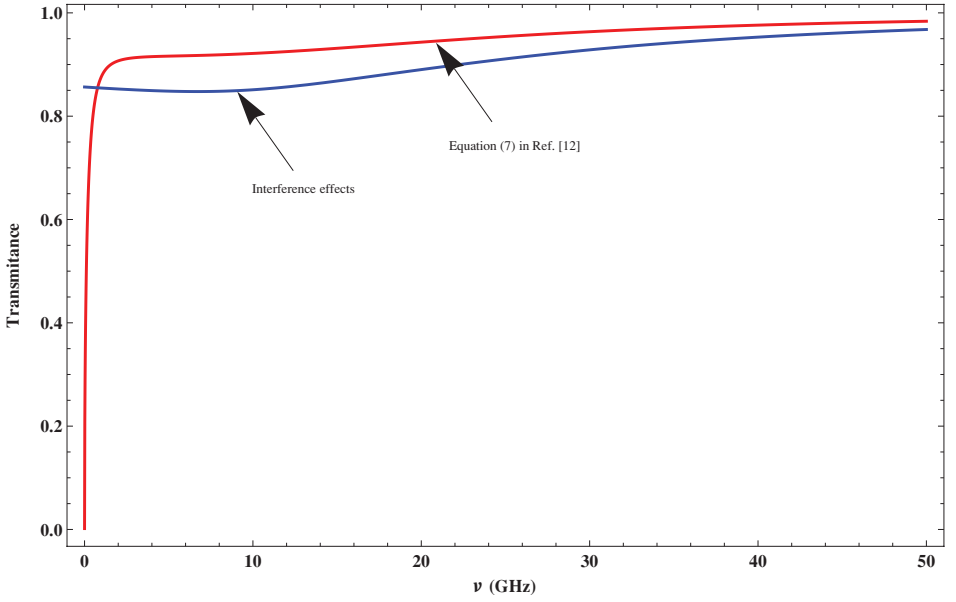

Figure 9. (Color online) Dependence of transmittance of hydrogen plasma slab on microwave frequency, when $n = 2.181 \times 10^{17}\mathrm{m}^{-3}$, $d = 1$ cm, and $\upsilon_e = 22$ GHz, from (7) in Ref. [12] and in the presence of interference effects.

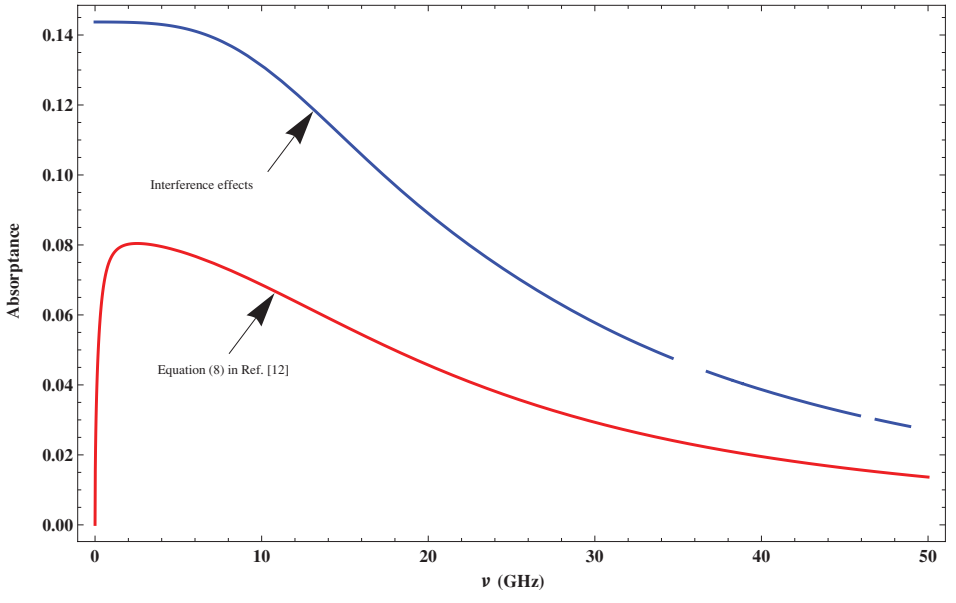

Figure 10. (Color online) Dependence of absorptance of hydrogen plasma slab on microwave frequency, when $n = 2.181 \times 10^{17}\ \mathrm{m}^{-3}$, $d = 1$ cm, and $\upsilon_e = 22$ GHz, from (8) in Ref. [12] and in the presence of interference effects.

https://doi.org/10.1017/S0022377811000018 Published online by Cambridge University Press

4. Conclusion

In this work, by considering the interference effects because of multiple reflections between thin plasma film interfaces, we investigated the behavior of the microwave propagation in a uniform hydrogen plasma film in the presence of CNTs. We obtained the reflectance, transmittance, and absorptance of microwave radiation at the plasma slab. We studied the effects of the continuously changing angle of propagation and plasma thickness with fixed parameters of the system on the absorbed, reflected, and transmitted powers of the system. It is found that the interference effects lead to a sinusoidal variation of the reflected intensity. In this way, one can see that in the present system the interference effects can greatly reduce the amount of reflection power, but the absorption power increases. Thus, in practice, a very thin hydrogen plasma film in the presence of CNTs could be tailored to act as an absorber of microwave radiation. Also, the numerical results show that for the present system, the TE and TM waves have largely indistinguishable microwave absorption and transmission spectrums.

In the present model, it is supposed that the density distribution of hydrogen plasma in the presence of CNTs is homogeneous. This condition requires that the fractional change in density distribution of plasma film in a distance of the order of a microwave wavelength must be much smaller than unity; consequently, for non-homogeneous mediums where density distribution along the film does not have an slowly varying behavior, our problem modified to a multilayered structure with N layers of different permittivity. This consequence will be reported somewhere else. Also, a future study will focus on the role of nonlinear effects on the electromagnetic response of the system [22].

References

[1] Li, Y. H. and Lue, J. T. 2007 *J. Nanosci. Nanotechnol.* **7**, 3185.

[2] Kong, J., Franklin, N. R., Zhou, C. W., Chapline, M. G., Peng, S., Cho, K. J. and Dai, H. J. 2000 *Science* **287**, 622.

[3] Ye, Z., Deering, W. D., Krokhin, A. and Roberts, J. A. 2006 *Phys. Rev.* B **74**, 075425.

[4] Imholt, T. J., Dyke, C. A., Hasslacher, B., Perez, J. M., Price, D. W., Roberts, J. A., Scott, J. B., Wadhawan, A., Ye, Z. and Tour, J. M. 2003 *Chem. Mater.* **15**, 3969.

[5] Yamanaka, S., Fujikane, M., Uno, M., Murakami, H. and Miura, O. 2004 *J. Alloys Compd.* **366**, 264.

[6] Dillon, A. C., Gilbert, K. E. H., Parilla, P. A., Alleman, J. L., Hornyak, G. L., Jones, K. M. and Heben, M. J. 2002 In: *Proceedings of the 2002 US DOE Hydrogen Program Review, NREL/CP-610-32405.*

[7] Wadhawan, A., Garret, D. and Perez, J. M. 2003 *Appl. Phys. Lett.* **83**, 2683.

[8] Naab, F., Dhoubhadel, M., Holland, W., Duggan, J., Roberts J. and McDaniel, F. 2004 In: *Proceedings of the 10th International Conference on Particle Induced X-ray Emission and Analytical Applications*, Portoroz, Slovenia, pp. 601, published electronically at http://pixe2004.ijs.si/proceedings

[9] Peng, Z., Peng, J. and Ou, Y. 2006 *Phys. Lett.* A **359**, 56.

[10] Peng, Z., Peng, J., Peng, Y., Ou, Y. and Ning, Y. 2008 *Physica* E **40**, 2400.

[11] Moradi, A. 2009 *Phys. Plasmas* **16**, 113501.

[12] Moradi, A. 2010 *Appl. Opt.* **49**, 1728.

[13] Moradi, A. 2010 *J. Appl. Phys.* **107**, 066104.

[14] Nikolaev, P., Bronikowski, M. J., Bradley, R. K., Rohmund, F., Colbert, D. T., Smith, K. A. and Smalley, R. E. 1999 *Chem. Phys. Lett*. **313**, 91.

[15] Bronikowski, M. J., Willis, P. A., Colbert, D. T., Smith, K. A. and Smalley, R. E. 2001 *J. Vac. Sci. Technol*. A **19**, 1800.

[16] Born, M. and Wolf, E. 1975 *Principles of Optics*, 5th edn. New York, NY: Pergamon Press.

[17] Yeh, P. 1998 *Optical Waves in Layered Media*. New Jersey: John Wiley and Sons.

[18] Stenzel, O. and Stendal, A. 1999 In: *Optical Properties in Wiley Encyclopedia of Electrical and Electronics Engineering*, Vol. 15 (ed. J. G. Webster), New York, NY: John Wiley and Sons.

[19] Jacob, W., Keudell, A. and Schwarz-Selinger, T. 2000 *Braz. J. Phys*. **30**, 508.

[20] Gradov, O. M. and Stenflo, L. 1983 *Phys. Rep*. **94**, 111.

[21] Brodin, G., Marklund, M., Stenflo, L. and Shukla, P. K. 2007 *Phys. Lett*. A **367**, 233.

[22] Shukla, P. K. and Stenflo, L. 2005 *Phys. Plasmas* **12**, 044503.